

J8.5 DEVELOPMENT OF A NEAR-REAL TIME HAIL DAMAGE SWATH IDENTIFICATION ALGORITHM FOR VEGETATION

Jordan R. Bell¹, Andrew L. Molthan², Lori A. Schultz³, Kevin M. McGrath⁴, Jason E. Burks²

¹Department of Atmospheric Science/NASA Short-term Prediction Research and Transition (SPoRT) Center, Huntsville, Alabama

²NASA SPoRT Center, Huntsville, Alabama

³University of Alabama in Huntsville/ESSC/NASA SPoRT, Huntsville, Alabama

⁴Jacobs, Inc. /NASA SPoRT Center, Huntsville, Alabama

1. INTRODUCTION

Every year in the Midwest and Great Plains, widespread greenness forms in conjunction with the latter part of the spring-summer growing season. This prevalent greenness forms as a result of the high concentration of agricultural areas having their crops reach their maturity before the fall harvest. This time of year also coincides with an enhanced hail frequency for the Great Plains (Cintineo et al. 2012). These severe thunderstorms can bring damaging winds and large hail that can result in damage to the surface vegetation. The spatial extent of the damage can be a relatively small concentrated area or be a vast swath of damage that is visible from space.

These large areas of damage have been well documented over the years. In the late 1960s aerial photography was used to evaluate crop damage caused by hail. As satellite remote sensing technology has evolved, the identification of these hail damage streaks has increased. Satellites have made it possible to view these streaks in additional spectrums. Parker et al. (2005) documented two streaks using the Moderate Resolution Imaging Spectroradiometer (MODIS) that occurred in South Dakota. He noted the potential impact that these streaks had on the surface temperature and associated surface fluxes that are impacted by a change in temperature. Gallo et al. (2012) examined the correlation between radar signatures and ground observations from storms that produced a hail damage swath in Central Iowa also using MODIS. Finally, Molthan et al. (2013) identified hail damage streaks through MODIS, Landsat-7, and SPOT observations of different resolutions for the development of a potential near-real time applications.

The manual analysis of hail damage streaks in satellite imagery is both tedious and time consuming, and may be inconsistent from event to

event. This study focuses on development of an objective and automatic algorithm to detect these areas of damage in a more efficient and timely manner. This study utilizes the MODIS sensor aboard the NASA Aqua satellite. Aqua was chosen due to an afternoon orbit over the United States when land surface temperatures are relatively warm and improve the contrast between damaged and undamaged areas. This orbit is also similar to the orbit of the Suomi-National Polar-orbiting Partnership (NPP) satellite. The Suomi NPP satellite hosts the Visible Infrared Imaging Radiometer Suite (VIIRS) instrument, which is the next generation of a MODIS-like sensor in polar orbit.

2. DATA

Data for this work comes from NASA's Land Processes Distributed Active Archive Center (LP-DAAC). The data that is stored in the LP-DAAC's data pool is easily accessible via an ftp website. The level 2 data is processed and projected onto a global sinusoidal grid. This makes it easy for an end user to select only areas that are needed for analysis.

The MYD09GQ product was used to create NDVI products for this study. This product provides the daily surface reflectance values for bands 1 (0.65 um red) and 2 (0.86 um near infrared). These 250 meter bands are the necessary bands required for computing NDVI.

This study also incorporates land surface temperature (LST) provided by the Level 3 MY11A1 product, derived from MODIS bands 31 (11.03 um thermal infrared) and 32 (12.02 um thermal infrared), with a spatial resolution of 1 kilometer. Quality indicators provided with each product were used to identify and remove clouds from each channel prior to work done in this study.

Multiple tiles of both products were needed for this case study and subsequent additional case studies. The MODIS Reprojection Tool (MRT) was used to combine multiple tiles and to provide nearest neighbor resampling of the 1 km LST tiles to 250 m to match the resolution of the NDVI generated products.

Hail occurrence was estimated from radar observations using the National Severe Storm Laboratory's (NSSL) Maximum Expected Size of Hail (MESH) product, which provides composited radar data over a grid. This 1 km by 1 km composite comes from the Hail Detection Algorithm (Witt et al. 1998) and was used to attempt to correlate degrees of damage with radar estimated hail size.

3. 18 AUGUST 2011 CASE STUDY

Various techniques were explored in this study to evaluate the effectiveness of using NDVI change and other approaches. This study evaluates three techniques using hail damage streaks following the 18 August 2011 hail event in the Central Plains previously examined by Molthan et al. (2013).

During the late evening of 18 August 2011 and into the early morning hours of 19 August 2011, severe thunderstorms with large hail and damaging winds moved from northeast Nebraska southeastward along the Missouri River and into southwestern Iowa and northwestern Missouri. These storms also had damaging winds associated with them per SPC Storm Reports (Fig 2a). According to the MESH product the largest radar indicated hail upwards in size of 12 cm, or ~5 in. (Figure 2b).

Figure 1 shows a true color MODIS image from morning of 25 August 2011 (reproduced from Molthan et al. 2013). The image shows three distinct areas of damaged vegetation that were a result of the severe thunderstorms. The area of damage just to the southeast of Yankton will not be analyzed in this paper, as this study focuses on two prominent areas of damage in southwestern Iowa are. These areas were chosen to be analyzed as they are much bigger than the one to the north. Colored boxes represent observations in the Molthan et al. (2013) study using other sensors with higher spatial resolution.

4. TECHNIQUES

4.1 NDVI Difference

The simplest method for detecting damage is producing an NDVI difference derived from NDVI values observed before and after the severe weather event. This type of analysis has been performed on several prominent hail damage streaks over the past decade (Molthan et al. 2013; Gallo et al. 2012; Parker et al. 2005). The primary objective of this technique is to examine quantitative trends between before storm imagery and after storm imagery. Figure 3a shows a 14-day NDVI composite valid on the afternoon of 18 August. This composite shows a very healthy vegetation signal with values across the domain well above 0.7. Urban areas and the Missouri River flooding are also noticeable as areas that have NDVI values of 0.0 or less.

Figure 3b shows a single day NDVI image taken the next afternoon on 19 August 2011. This snapshot shows just a few clouds in the middle of the image. This scene also shows two faint streaks on the Iowa-Missouri border. These streaks appear to be the result of high winds and large damaging hail associated with the overnight storms. These streaks appear to have NDVI values in the range of 0.4 to 0.6, or a significant reduction from just 24 hours prior. Figure 3c shows this 1 day difference is very apparent. The two streaks that were noticeable in Figure 3b, stand out much more now. Most of the areas in the streak experienced a NDVI change of -0.2 to -0.4

To investigate the relationship between radar-estimated hail size and vegetation damage (NDVI change), a box and whiskers plot was created (Figure 3d). This analysis shows that there was little to no change in NDVI for areas that saw radar estimated hail sizes between 2.54 cm (1.00 in.) and 5.08 cm (2.00 in.). Once the radar estimated hail was estimated to be over 5.08 cm, a downward trend in median values of each bin is apparent. This downward signal grows stronger as the vegetation continues to weaken and wilt with later observations (not shown). It is important to remember that radar estimated hail sizes are calculated above the ground and from reflectivity measured at the beam height. Surface reports of hail size may differ from what is actually observed at the ground due to melting or other radar sampling factors.

4.2 Vegetation Health Index (VHI)

The analysis of hail streaks by Parker et al. (2005) identified an increase in land surface temperature in and around damaged areas of vegetation. The increase in land surface temperature is a result of the decreased albedo in the damaged area, allowing for more solar radiation to be absorbed by the surface. Based upon their results, land surface temperature may also provide information leading to improved detection of damage areas. This study evaluates the use of the Vegetation Health Index (VHI, Kogan 2001) as a means of identifying damage areas. The VHI was originally developed to monitor vegetation for stress due to drought conditions. VHI is comprised of two indices, the Vegetation Condition Index (VCI), based upon NDVI, and the Temperature Condition Index (TCI), based upon brightness temperature, and are combined to create the VHI. These indices are calculated using multi-year minimums, means, and maximums of NDVI and land surface temperatures.

$$VCI = 100 * \frac{NDVI_{mean} - NDVI_{min}}{NDVI_{max} - NDVI_{min}} \quad (1)$$

$$TCI = 100 * \frac{BT_{max} - BT_{mean}}{BT_{max} - BT_{min}} \quad (2)$$

$$VHI = 0.5(VCI) + 0.5(TCI) \quad (3)$$

Because this work focuses on short term changes to vegetation, uses land surface temperature, and the vegetation pattern can vary from year to year, Kogan's original equations were modified. This modification allows for the indices to be computed on a much shorter time scale. Instead of using multi-year minimums, means, and maximums, 14-day 10th, 50th and 90th percentiles were used:

$$VCI = 100 * \frac{NDVI_{50} - NDVI_{10}}{NDVI_{90} - NDVI_{10}} \quad (4)$$

$$TCI = 100 * \frac{LST_{90} - LST_{50}}{LST_{90} - LST_{10}} \quad (5)$$

$$VHI = 0.6(VCI) + 0.4(TCI) \quad (6)$$

The inclusion of land surface temperature aids in the detection of potential damage. For VCI, TCI, and VHI, lower values indicate vegetation stress. Figure 4a shows the 14 day VCI valid on 31 August 2011, with the same two major streaks apparent on the Iowa-Missouri border. VHI values in these damage streaks appear to be well below

30. However, now there appears to be a smaller third streak to the west of the big streaks and to the east of the Missouri River. The radar estimate of hail shows a small streak of hail to the west of the primary tracks. The two primary tracks are well defined in the TCI product (Fig. 4b) but the third streak is not as well defined. When combining the two indices into the final index, all three damage streaks are very apparent (Fig. 4c).

The VHI shows a healthier vegetation signal (green) west of the two main hail damage streaks in Nebraska and a stressed vegetation signal (red) in Iowa, to the east of the hail damage streaks. It is highly plausible that the reason behind these signals, despite a well uniform signal in Figure 3a is due to clouds and cloud shadows that were not completely eliminated using the MODIS cloud mask. Cloud and cloud shadow detection must be improved to ensure that they do not produce errors in composites of NDVI and LST. In addition, this procedure would benefit from increased numbers of observations because this modified approach is using percentiles, greater numbers of observations will improve the results. In order to increase the samples for this product potential solutions include increasing the number of satellites being used for the product (i.e. Terra-MODIS, Suomi-NPP VIIRS) or increase the number days that are being included in the sampling by just Aqua-MODIS (i.e. 14 days vs. 28 days). Future work will examine which improvement yields the best results.

4.3 Feature Detection/Extraction

Image classification provides another potential methodology for detecting hail damage in vegetation. There are both supervised and unsupervised techniques that can be used to help detect features in imagery and/or extract those features. This study uses an unsupervised methodology to identify and extract areas of potential areas of damage.

In order to detect these areas, both single day NDVI and LST single day is analyzed for anomalies. Using the same NDVI image from 19 August 2011 (Fig 5a) as before, anomalies were calculated for each pixel in the image. The anomalies are calculated using a moving that is centered on each pixel. The anomalies are the difference between the center pixel and the median value of the remaining pixels in the moving box.

The NDVI anomaly image (Fig. 5c), like the other techniques, shows the two main hail damage streaks. The two main hail damage streaks appear to have NDVI values of -0.1 to -0.3 below the median. The rest of the image is noisy, but the noise is scattered rather uniformly, which could just be minor NDVI changes that result from differences in viewing angle or other slight differences. The same technique is applied to the land surface temperature scene. Within the damage streaks, LST anomalies of the streak are 2 to 4 Kelvin warmer than the local background (Fig. 5d). There is also much less noise observed in the land surface temperature anomaly product outside the damage streaks.

NDVI and LST anomalies can be combined in a classification approach to identify damaged pixels. For this work, Otsu's method was selected (Otsu 1975). The Otsu technique converts anomaly values to a grayscale image, and the technique sorts each pixel based on into two categories: background or anomaly. This results in a mask where each pixel is categorized as either 0 (background) or 1 (anomaly). Figure 5e shows areas identified as anomalies in both the NDVI and LST. The two hail streaks are present but there are still several areas identified outside of the hail-damaged area. This noise can be attributed to urban areas, early harvest and issues resulting from clouds and cloud shadows. To limit returns to areas with possible hail damage, MESH was used to extract areas that experienced radar-estimated hail greater than 2.54 cm (1 in.) (Fig. 5f). By doing this, much of the noise is eliminated. Features outside of the primary streaks are also identified as possible damage areas.

5. SUMMARY / FUTURE WORK

This paper outlines the methodology being developed to automatically detect vegetation damage as a result of severe thunderstorms that bring large hail and damaging winds. Previous identification of these damaged areas had been manually done, in a non-efficient manner. The techniques that are explored here range from simple NDVI differencing to incorporating land surface temperature data with NDVI in the Vegetation Health Index, to feature detection and extraction. Each of these techniques have their strengths and weaknesses. Additional cases studies and analysis will be performed.

From these additional case studies, each individual method will be evaluated tuned to provide its best performance. Each technique and its performance will then be evaluated over the course of several previous growing seasons to simulate near-real time conditions. During these simulated near-time conditions, additional datasets, such as land cover and crop type will be integrated as well.

Skill scores and validation will be compiled during season long tests. Skill scores will help determine the exact make-up of the final algorithm, prior to generation of a near-real time product. This product will be available to end users that will benefit from such product. The target end users are those who work to perform storm surveys and those who utilize the NOAA/NWS Damage Assessment Toolkit.

6. REFERENCES

- Changnon, S. A., and N. A. Barron, 1971: Quantification of Crop-Hail Losses by Aerial Photography. *J. Appl. Meteorol.*, **10**, 86–96, doi:10.1175/1520-0450(1971)010<0086:QOCHLB>2.0.CO;2. <http://journals.ametsoc.org/doi/abs/10.1175/1520-0450%281971%29010%3C0086%3AQOCHLB%3E2.0.CO%3B2> (Accessed November 2, 2014).
- Cintineo, J. L., T. M. Smith, V. Lakshmanan, H. E. Brooks, and K. L. Ortega, 2012: An Objective High-Resolution Hail Climatology of the Contiguous United States. *Weather Forecast.*, **27**, 1235–1248, doi:10.1175/WAF-D-11-00151.1. <http://dx.doi.org/10.1175/WAF-D-11-00151.1>.
- Gallo, K., T. Smith, K. Jungbluth, and P. Schumacher, 2012: Hail Swaths Observed from Satellite Data and Their Relation to Radar and Surface-Based Observations: A Case Study from Iowa in 2009. *Weather Forecast.*, **27**, 796–802, doi:10.1175/WAF-D-11-00118.1. <http://journals.ametsoc.org/doi/abs/10.1175/WAF-D-11-00118.1> (Accessed December 18, 2013).
- Molthan, A., J. Burks, K. McGrath, and F. LaFontaine, 2013: Multi-sensor examination of hail damage swaths for near real-time

- applications and assessment. *J. Oper. Meteorol.*, **1**, 144–156, doi:10.15191/nwajom.2013.0113. <http://www.nwas.org/jom/abstracts/2013/2013-JOM13/abstract.php> (Accessed November 2, 2014).
- Otsu, N., 1975: A threshold selection method from gray-level histograms. *Automatica*, **11**, 23–27.
- Parker, M. D., I. C. Ratcliffe, and G. M. Henebry, 2005: The July 2003 Dakota Hailswaths: Creation, Characteristics, and Possible Impacts. *Mon. Weather Rev.*, **133**, 1241–1260, doi:10.1175/MWR2914.1.
- <http://journals.ametsoc.org/doi/abs/10.1175/MWR2914.1> (Accessed October 28, 2014).
- Witt, A., M. D. Eilts, G. J. Stumpf, J. T. Johnson, E. D. W. Mitchell, and K. W. Thomas, 1998: An Enhanced Hail Detection Algorithm for the WSR-88D. *Weather Forecast.*, **13**, 286–303, doi:10.1175/1520-0434(1998)013<0286:AEHDAF>2.0.CO;2. [http://journals.ametsoc.org/doi/abs/10.1175/1520-0434\(1998\)013<0286:AEHDAF>2.0.CO;2](http://journals.ametsoc.org/doi/abs/10.1175/1520-0434(1998)013<0286:AEHDAF>2.0.CO;2) (Accessed January 10, 2015).

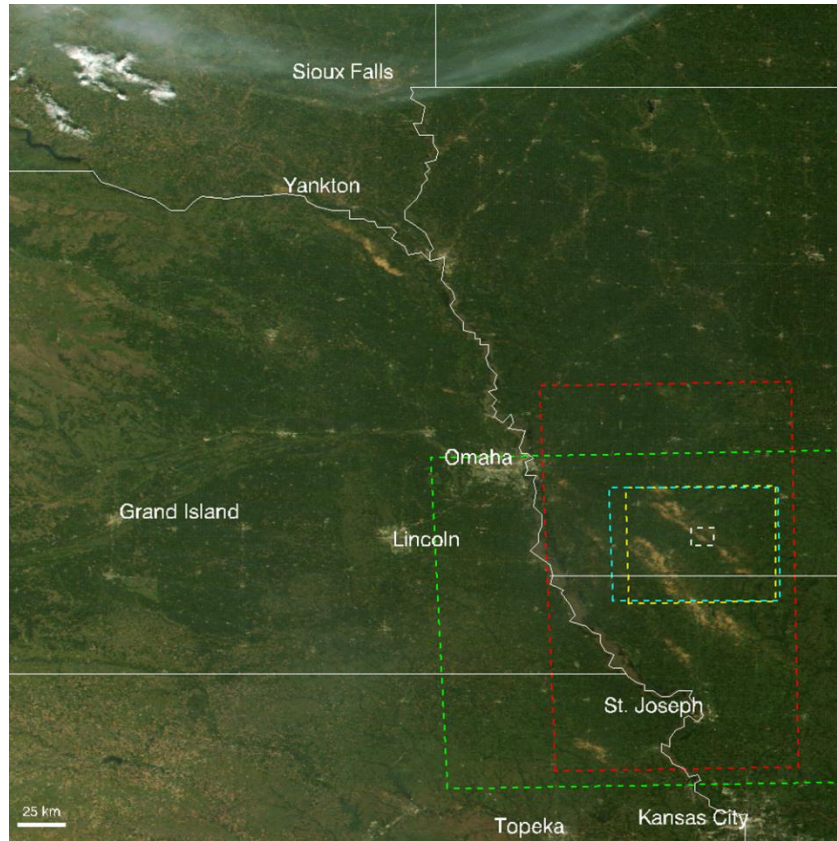


Figure 1. True color MODIS image from 25 August 2011 showing damage that was a result of damaging winds and large hail that occurred on 18 August 2011. Image reproduced from Molthan et al. (2013).

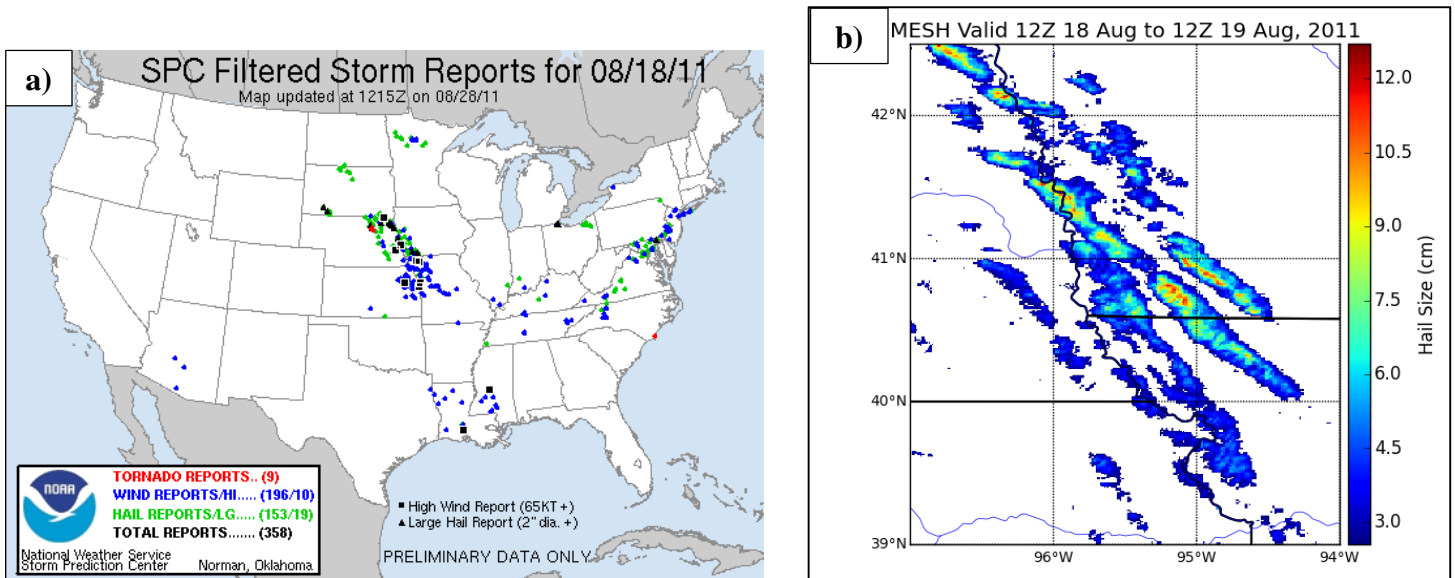


Figure 2. The impact of severe thunderstorms during the overnight hours of the 18 August 2011 into the morning of 19 August 2011. (a) Storm Prediction Center storm reports for the 18 August 2011. (b) Maximum Expected Size of Hail valid 12z 18 August 2011 to 12z 19 August 2011.

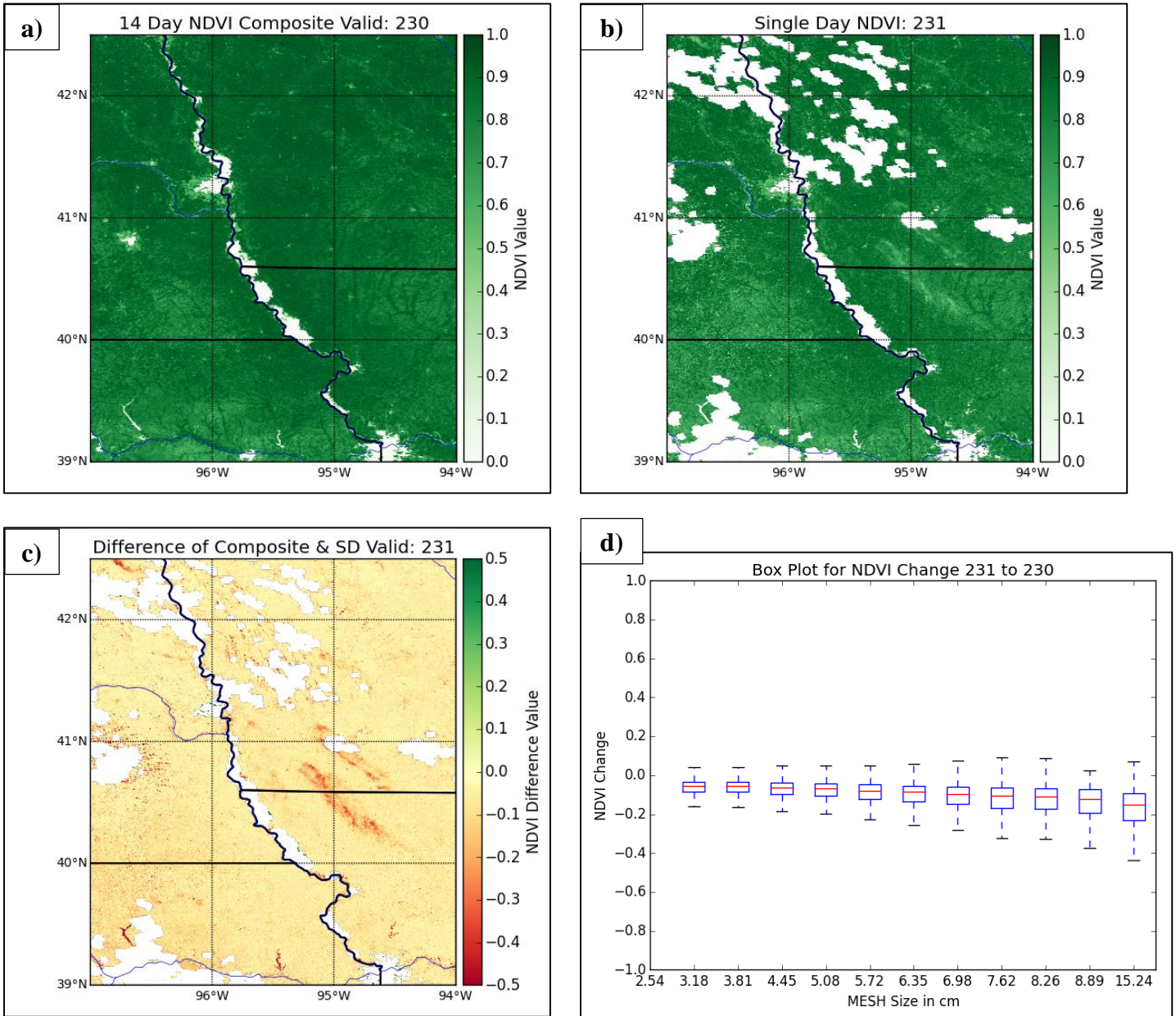


Figure 3. (a) 14 day NDVI composite valid for the 18 August 2011. (b) Single day NDVI image valid for 19 August 2011. (c) NDVI difference between single day image (b) and composite (a). (d) Box and whisker plot showing NDVI difference for various MESH size categories.

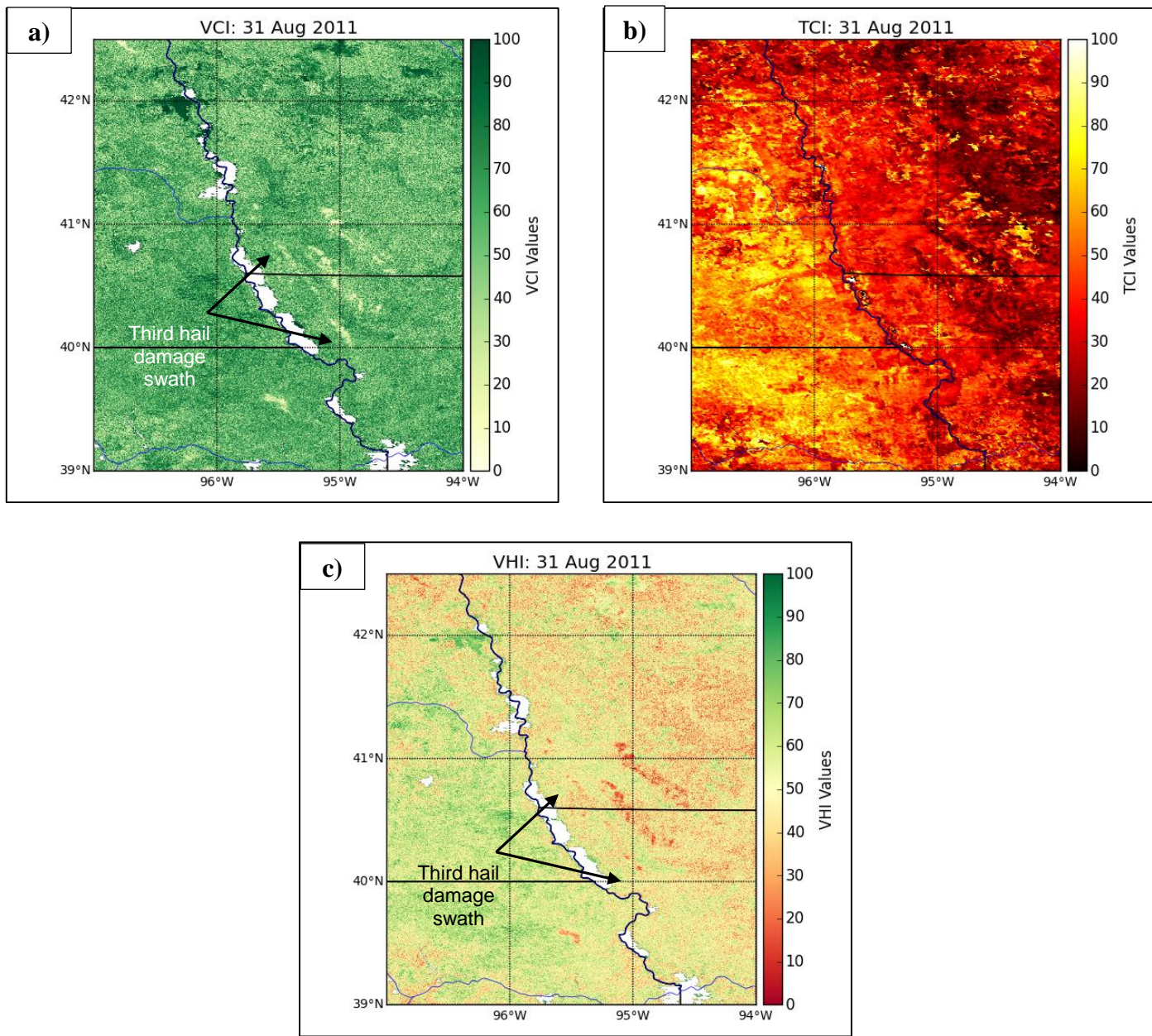


Figure 4. (a) Vegetation Condition Index (VCI) valid for 31 August 2011 and identification of an additional hail damage streak. (b) Temperature Condition Index (TCI) valid for 31 August 2011. The third hail damage streak is not as visible. (c) Vegetation Health Index (VHI) valid for 31 August 2011. Third hail damage streak is faint but apparent.

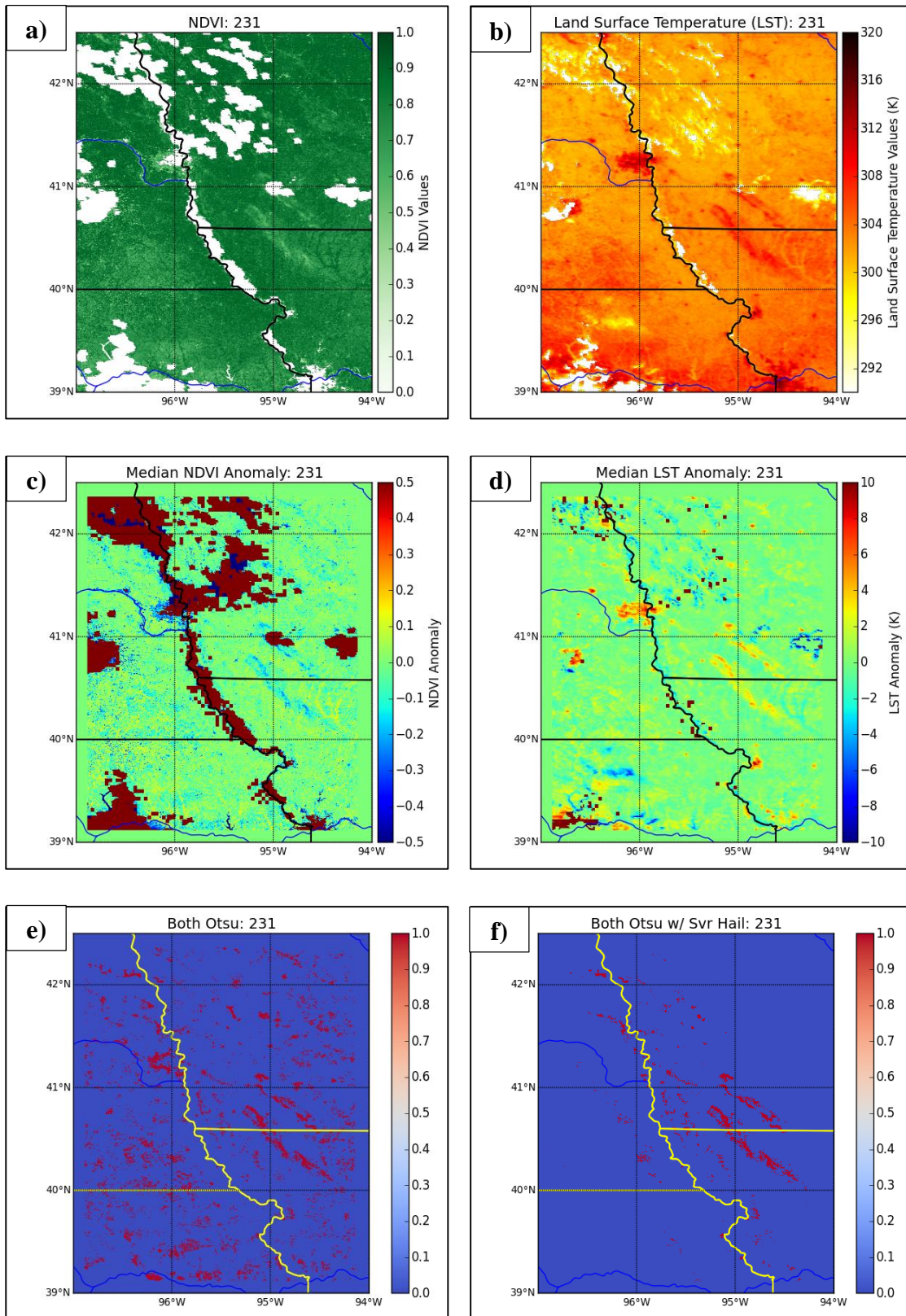


Figure 5. (a) Single day NDVI image acquired from Aqua-MODIS on 19 August 2011. (b) Single day land surface temperature (LST) image acquired by Aqua-MODIS on 19 August 2011. (c) Median NDVI Anomaly of (a). (d) Median LST anomaly of (b). (e) Image shows the results of Otsu's filter that is positive in both median NDVI image (c) and LST image (d). (f) Noise reduced by using MESH to show only areas that experienced hail.